



Crashworthiness Investigation of Multi-stage Structures Designed for Underrun Protection Devices

Tongchana Thongtip

Department of Teacher Training in Mechanical Engineering, Faculty of Technical Education, King Mongkut's University of Technology North Bangkok, Bangkok, Thailand

Saharat Chanthanumataporn*

Department of Mechanical and Automotive Engineering, The Sirindhorn International Thai-German Graduate School of Engineering (TGGS), King Mongkut's University of Technology North Bangkok, Bangkok, Thailand

* Corresponding author. E-mail: saharat.c@tggs.kmutnb.ac.th DOI: 10.14416/j.asep.2020.10.003

Received: 6 May 2020; Revised: 29 June 2020; Accepted: 20 July 2020; Published online: 15 October 2020

© 2021 King Mongkut's University of Technology North Bangkok. All Rights Reserved.

Abstract

Due to the disparity between large trucks and passenger vehicles, most deaths in large truck crashes are occupants in small cars, which under-ride the large truck. To protect the under-riding of small vehicles during crash and mitigate the severity, various designs of underrun protection devices have been developed to be installed at the front, side, rear of trucks. Not only can underrun protection devices protect a small vehicle from under-riding a truck, but also minimize the severity of crash to develop crashworthiness. In this paper, various cross section patterns of underrun protection device guard bar are designed with the aims to improve the crashworthiness. Moreover, the crashworthiness capability is clarified for future design guideline. The proposed structural configuration is designed from the concept of multi-stage energy absorption, which also results in an improvement of bending stiffness. To investigate the crashworthiness of the proposed design, the dynamic analysis is performed in LS-DYNA explicit commercial finite element analysis package. The guard bar is cut partially and investigated by performing drop impact test. Energy absorption, specific energy absorption, peak impact force, crash force efficiency, and stroke efficiency are considered as quantitative criteria for crashworthiness evaluation. The technique of order of preference by similarity to ideal solution is adopted to perform a multi-criteria decision analysis and identify the overall performance score of each design. The results indicate that the triple stage UPD guard bar yields the best performance score and improve the overall crashworthiness score up to 10% as compared with the rectangular design of standard UPD guard bar.

Keywords: Crashworthiness, Impact test, TOPSIS

1 Introduction

Based on the yearly report of World Health Organization (WHO), over 1.35 million people die and road traffic injuries are now the leading killer of people aged 5–29 years [1], [2]. The 2017 statistics report of Insurance Institute for Highway Safety (IIHS) also points out that

97% of people deaths in large truck crashes are small vehicle occupants because large trucks have more weight than passenger cars have up to 20–30 times and trucks also have considerable ground clearance. Thus, smaller vehicles can easily underride trucks in crash accident [3]. The underride phenomenon causes serious and fatal injuries for small vehicle occupants

Please cite this article as: T. Thongtip and S. Chanthanumataporn, "Crashworthiness investigation of multi-stage structures designed for underrun protection devices," *Applied Science and Engineering Progress*, vol. 14, no. 3, pp. 328–337, Jul.–Sep. 2021, doi: 10.14416/j.asep.2020.10.003.

owing to the intrusion of the passenger compartment since trucks structure are higher than the crash zones of the small vehicle [4], [5]. Moreover, the reason of large mass discrepancy results in the severe impact force transferred to smaller vehicle. Therefore, when a smaller vehicle crashes a truck, serious or fatal injury can result to small vehicle occupants [6].

To protect a under riding crash of small vehicles, various underrun protection devices was invented and enforced to be installed on the front, side, and rear-end of trucks. In European Union, the legislation determines that trucks manufactured after 2004 must be installed an underrun protection device in the front [7]. In the incident of a truck head-on collision with a car, the frontal underrun protection device (FUPD) must be able to stop the car from going under the truck and absorb crash energy. The frontal underrun protection device usually consists of a transverse horizontal beam so called guard bar and its support structure as shown in Figure 1(a). The geometric of FUPD and a static force level that the FUPD must endure to satisfy its functionality are regulated by UNECE R93. For side protection device as shown in Figure 1(b), its functionality is not only to protect cars from under riding but also to prevent motorcyclists, cyclists, and pedestrians from falling under the truck and being crushed by the rear wheels. The standard geometrical and technical requirements for side guards are regulated by UNECE R73. For the case of trucks rear-end, the utilization of rear underrun protection device (RUPD) as shown in Figure 1(c) has been introduced by many countries around the world with the hope to enhance the compatibility between trucks and small vehicles. In addition, each country has utilized their own standard, for instance, FMVSS 223/224 in USA, CMVSS 223 in Canada, UNECE R58 in Europe, GB11567.2-2001 in china, and IS 14812-2005 in India [8]–[13].

Various research on underrun protection device have been proposed to improve crashworthiness for car to truck collisions. The crashworthiness indicators, usually considered, are the energy absorption capability and crashing force. Many researches concentrate on the improvement of energy absorption capability and the minimization of crashing force resulting in the reduction of passenger injuries. For FUPD, there are several efforts to improve the crashworthiness results. For instance, Framby and Lantz [14] try to improve

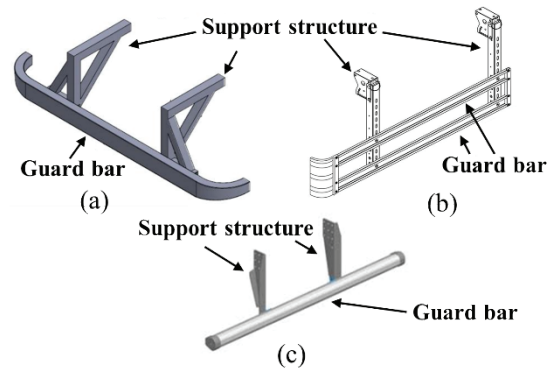


Figure 1: Schematic drawing of (a) frontal underrun protection device (b) side protection device (c) rear underrun protection device.

the energy absorbing capability of a FUPD and study its robustness and reliability. The results show the improved FUPD are rather non-robust and unreliable, but it can protect a passenger car from underrunning. However, for the case of overlap crash, the FUPD is not stiff enough. For side underride protection device, Patrick [15] develops side underride protection devices based on a topology and multi-objective optimization design approach. For the RUPD, Liu Hong-fei *et al.* and Al-Bahash *et al.* [13], [16] design the protection bar comprising of circular tubes sandwiched between two steel plates. In the circular tubes, aluminum foam is filled with the aim to increase energy absorption. Several research [17], [18] try to improve the absorption capability of RUPD support structure. The improvement is performed by designing the support structure hinged onto the chassis frame and installing the energy absorbing crush tubes between the support structure and the chassis frame. It can be concluded from the literature review that the improvement of strength and crashworthiness reliability is the important issue that should be considered for the development of underrun protection device.

In this paper, the concept idea of multi-stage UPD guard bars is proposed to improve the strength and crashworthiness reliability. In the view of strength, the enhancement of multi-stage UPD guard can be answered based on the principle of mechanics that the flexural stiffness of a beam can be improved by thickening its structure. However, there is no principal that can answer the crashworthiness development of multi-stage UPD guard. Thus, the crashworthiness

of the proposed design is investigated by performing drop impact test and considering the important crashworthiness criteria of energy absorption, specific energy absorption, peak impact force, crash force efficiency, and stroke efficiency. After impact test, the technique of order of preference by similarity to ideal solution is adopted to perform a multi-criteria decision analysis and clearly clarify the overall performance score of each design.

2 Design of Multi-stage UPD

The structural design of a standard UPD guard bar is generally rectangular or circular cross-section shape, sometimes resulting in low performance of crashworthiness and strength reliability. In this paper, the concept multi-stage structure is proposed to apply for the UPD guard bar and the improvement of crashworthiness is investigated. Four designs of UPD guard bar and their mass are presented in Table 1, in which there are the general one stage with rectangular cross section, one stage with semicircle cross section, double stage, and triple stage. For double and triple

stage, the outer part is designed to be round shape with the hope to avoid the sharpness hazard. The structural material is mild steel (ASTM A36) and the material properties are concluded in Table 2.

3 Finite Element Model for Drop Impact Simulation

To investigate the crashworthiness improvement of the proposed multi-stage design, the most efficient dynamic drop impact technique is adopted [19]–[22]. In this study, the UPD guard bar is cut partially, and the dynamic drop impact tests are performed in LS-DYNA explicit commercial finite element analysis package.

The finite element model is composed of a specimen of UPD guard bar, the rigid fixture, and the impactor as shown in Figure 2. The specimens are modelled with 4-node shell elements with 5-integration points through the thickness, the LS-DYNA default Belytshko-Tsay formulation. The rigid fixture and the impactor are modelled with 8-node solid elements, with 1-integration point, the default constant stress solid element formulation. The shell element is employed with element size of 9×9 mm. The solid element

Table 1: Design of UPD guard bar

Design	1. Rectangular Guard Bar	2. Semicircle Guard Bar	3. Double stage Guard Bar	4. Triple stage Guard Bar
Isometric view				
Front view				
Mass	1.01 kg	1.01 kg	1.62 kg	2.24 kg

Table 2: Material properties for multi-stage UPD

Material	Young Modulus	Density	Yield Stress	Poisson's Ratio
A36 steel	210 GPa	7.85×10^{-6} kg/mm ³	200 MPa	0.3

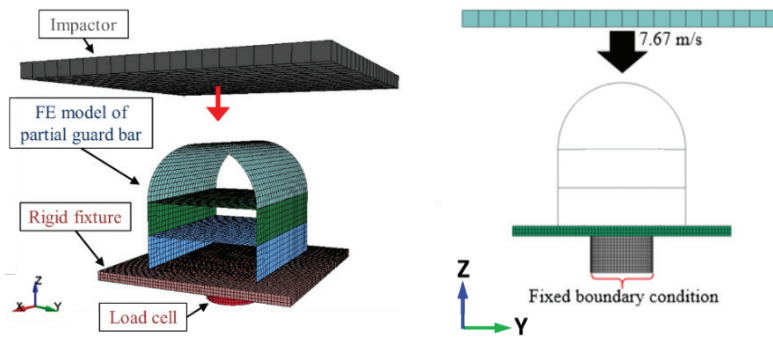


Figure 2: FE model for drop impact simulation.

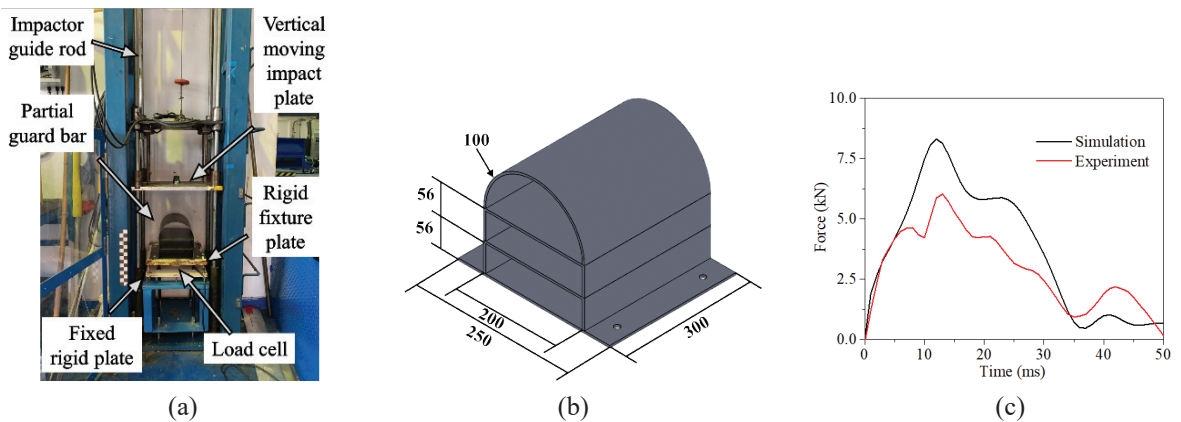


Figure 3: (a) Drop impact experiment (b) Dimension of specimen (c) Comparison of experimental and simulation results.

mesh sizes are $25 \times 25 \times 25$ mm for the impactor and $5 \times 5 \times 5$ mm for the fixture. The mesh size taken is verified from convergence studies. About the boundary condition of the model as shown in Figure 2, the partial part of guard bar is fixed on a rigid fixture and impacted by a vertically moving rigid plate. The rigid fixture is constrained in all degrees of freedom. The impactor with mass of 16 kg is free only the vertical translation, in which the initial impact velocity is 7.67 m/s corresponding to the drop height of 3 m in Z-direction.

The finite element model is verified from the drop impact experiments as shown in Figure 3. The experiment is conducted on the partial portion of guard bar using free-fall drop machine as displayed in Figure 3(a), in which the test condition is the same as the finite element model. The dimension of the specimen is presented in Figure 3(b), in which the length of experimental specimen is 50 mm longer than that of FE

one. The material properties are as same as described in Table 2. During the impact test, the specimen is fixed on the rigid fixture placed on the load cell and then an impact mass of 16 kg is dropped to impact the specimen. The drop height is set at 3 m as same as the finite element model. The variations of force are measured by load cell and the displacement is recorded by high speed camera. With the same condition of impact test, the comparison of experimental and simulation result of the force–time responses is presented in Figure 3(c). From the comparison, there are some difference of impact force amplitude because at the same drop height, the experimental impact velocity, measure by high speed camera, is lower than the simulation impact velocity, 7.67 m/s. The lower impact velocity results in the lower impact force. The error of experimental impact velocity is due to the friction of four impactor guide rods. However, the experimental and simulation results still show good agreement. By

this reason, the validity of the simulation model has been proven.

4 Crashworthiness Indicator

The capability of safety structures to absorb impact energy and to protect passengers during an accident incidence is known as “Crashworthiness”. Quantitative criteria such as energy absorption (EA), specific energy absorption (SEA), peak crushing force (F_{max}), crash force efficiency (CFE), and stroke efficiency (SE) are frequently used to evaluate the crashworthiness performance. The energy absorption can be formulated as follows [Equation (1)]:

$$EA(\delta) = \int_0^{\delta} F(x)dx \quad (1)$$

where, δ is the collision displacement and $F(x)$ is variation of force versus displacement.

To compare the energy absorption with different materials or structures, the term of structural mass is considered, and the energy absorbed per unit mass is defined as the specific energy absorption. [Equation (2)]

$$SEA(\delta) = \frac{EA(\delta)}{mass} \quad (2)$$

Additional parameter is F_{max} , which is the maximum reaction force generated by absorber structure. This force should be at a low and constant level during crash energy absorption. The parameter that indicate the consistency of F_{max} is Crash force efficiency (CFE), the ratio between mean and peak crash force. A good energy absorber that have less variation between mean force and peak force can yield CFE as close as one. [Equation (3)]

$$CFE = \frac{F_{avg}(\delta)}{F_{max}} \quad (3)$$

where, $F_{avg}(\delta)$ is the average force curve, which is defined as follows [Equation (4)]:

$$F_{avg}(\delta) = \frac{EA(\delta)}{\delta} \quad (4)$$

The next parameter is stroke efficiency (SE), the ratio between maximum collision displacement (δ) and the original height of the absorbing structure. High

value of SE indicates the efficient use of absorbing structure. [Equation (5)]

$$SE = \frac{\delta}{h} \quad (5)$$

5 Multiple Attribute Decision Making

As discussed above, there are many indicators for crashworthiness evaluation. Therefore, the technique of order of preference by similarity to ideal solution (TOPSIS) [23]–[25], a multi-criteria decision analysis method is adopted to identify the ranking of each design. TOPSIS consists of six steps as follows:

Step 1. Construct the decision matrix X_{ij} [Equation (6)]

$$X_{ij} = \begin{bmatrix} x_{11} & x_{12} & \cdots & x_{1n} \\ x_{21} & x_{22} & & x_{2n} \\ \vdots & \vdots & \vdots & \vdots \\ x_{m1} & x_{m2} & \cdots & x_{mn} \end{bmatrix} \quad (6)$$

where, m is alternative and n is criteria in this matrix. X_{ij} is the value of the alternative i with respect to the criterion j .

Step 2. Construct the normalized decision matrix R_{ij} as [Equation (7)]

$$R_{ij} = \begin{bmatrix} r_{11} & r_{12} & \cdots & r_{1n} \\ r_{21} & r_{22} & & r_{2n} \\ \vdots & \vdots & \vdots & \vdots \\ r_{m1} & r_{m2} & \cdots & r_{mn} \end{bmatrix} \quad (7)$$

where, $r_{ij} = \frac{x_{ij}}{\sqrt{\sum x_{ij}^2}}$ for $i = 1, \dots, m; j = 1, \dots, n$. This

step transforms various dimensional criteria into non-dimensional criteria, which allows comparisons between the criteria.

Step 3. Construct the weighted normalized decision matrix V_{ij} as [Equation (8)]

$$V_{ij} = \begin{bmatrix} w_1 r_{11} & w_2 r_{12} & \cdots & w_n r_{1n} \\ w_1 r_{21} & w_2 r_{22} & & w_n r_{2n} \\ \vdots & \vdots & \vdots & \vdots \\ w_1 r_{m1} & w_2 r_{m2} & \cdots & w_n r_{mn} \end{bmatrix} \quad (8)$$

where, w_i (for $i = 1, \dots, n$) is the weight of each criterion and is determined such that the important criterion takes a higher value; moreover, $\sum_{i=1}^n w_i = 1$

Step 4. Determine the ideal best and ideal worst. The positive ideal solutions as [Equation (9)]

$$V_j^+ = \{v_1^+, \dots, v_n^+\} \tag{9}$$

where, $v_j^+ = [\max (v_{ij}) \text{ if } j \in J^+; \min (v_{ij}) \text{ if } j \in J^-]$. Moreover, J^+ is the set of positive criteria (more is better) and J^- is the set of negative criteria (less is better). The negative ideal solution is [Equation (10)]

$$V_j^- = \{v_1^-, \dots, v_n^-\} \tag{10}$$

where, $v_j^- = [\min (v_{ij}) \text{ if } j \in J^+; \max (v_{ij}) \text{ if } j \in J^-]$.

Step 5. Calculate the Euclidean distance measure for each alternative. The Euclidean distance from ideal best is [Equation (11)]

$$S_i^+ = \left[\sum_{j=1}^m (V_j^+ - V_{ij})^2 \right]^{1/2}, i = 1, \dots, m \tag{11}$$

Correspondingly, the Euclidean distance from ideal best is [Equation (12)]

$$S_i^- = \left[\sum_{j=1}^m (V_j^- - V_{ij})^2 \right]^{1/2}, i = 1, \dots, m \tag{12}$$

Step 6. Calculate the performance score to the ideal solution P_i as [Equation (13)]

$$P_i = \frac{S_i^-}{S_i^+ + S_i^-}, 0 < P_i < 1 \tag{13}$$

Afterwards, select the performance score with P_i closest to 1 or the highest score for consider the ranking by the first rank is the better choice.

6 Results and Discussion

After the drop impact test of the UPD guard bars, presented in Table 2, have been conducted, the deformation results of each design are summarized in Table 3. In addition, the crashworthiness results of energy absorption (EA), specific energy absorption (SEA), maximum crash force (F_{max}), crash force efficiency (CFE), structural deformation, and stroke efficiency (SE) are presented in Figure 4. From the results, the design of triple stage UPD guard bar absorbs more impact energy than other designs do, and the double stage absorbs more energy than the design of rectangular and semicircle do. However, the design of semicircle shows lower energy absorbing capability than the design of rectangular does. These results indicate that the design with round shape outer part can absorb less amount of energy than the design with flat shape outer part since the flat shape has more contact area than the round design. Nonetheless, when considering the absorbed energy defined per unit mass as shown in Figure 4(b), the rectangular UPD guard bar still shows the highest specific energy absorption among other design due to its lowest mass. The semicircle UPD guard bar shows the lower specific energy absorption than the rectangular UPD guard bar does because of its lower energy absorption. Although the increment of structural stage can improve the energy absorbing capability, it can yield some negative results as shown in Figure 4(b). The results

Table 3: Deformation results of the partial cross bar

Design	1. Rectangular Guard Bar	2. Semicircle Guard Bar	3. Double Stages Guard Bar	4. Triple Stages Guard Bar
Isometric view				
Front view				
Deformation	29.18 mm	94.86 mm	119.83 mm	198.79 mm

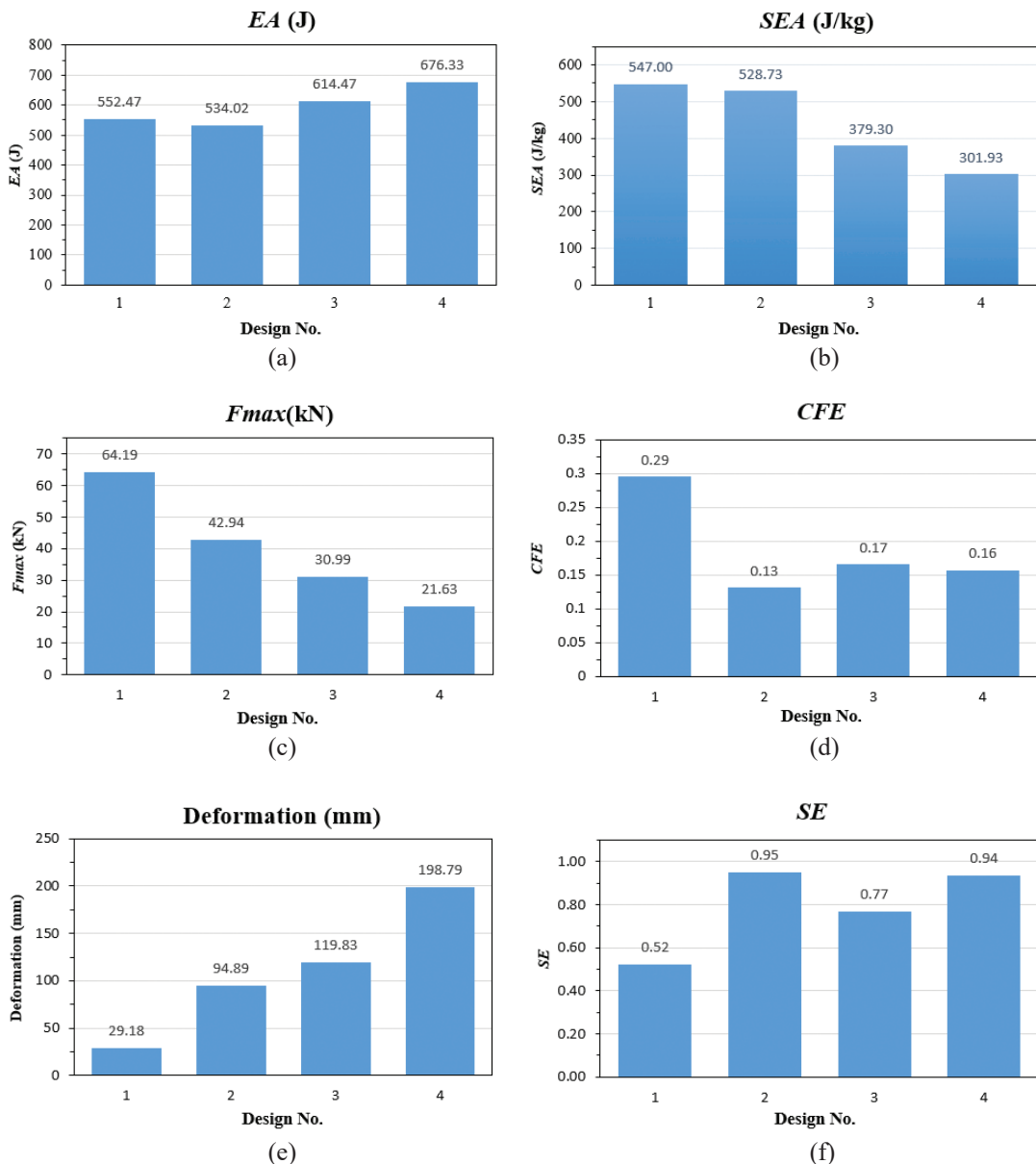


Figure 4: Crashworthiness indicators: (a) EA (b) SEA (c) F_{max} (d) CFE (e) Deformation (f) SE .

show that while the number of stages increases, the specific energy absorption trends to decrease because of the increment of its mass. Other than the energy absorption criteria, the peak crash force (F_{max}) is a significant indicator for the safety of the passengers that should be controlled in a small value. In Figure 4(c), the peak crash force (F_{max}) trends to decrease with the increase of the number of stages. Although the

rectangular UPD guard bar offers the best specific energy absorption, it shows the worst peak crash force, almost 50% higher than F_{max} of semicircle UPD guard bar. These results indicate that the design with round shape outer part and the increment of the number of stages can significantly minimize the peak crash force (F_{max}). For the crash force efficiency (CFE), the rectangular design shows the highest value whereas

other three designs show a bit variation between mean force and peak crash force. Although the high value of *CFE* indicates the good performance of absorbing structure, in this case, the higher *CFE* value of rectangular design results from the lower structural deformation and the higher average force as compared with those of other designs. As shown in Figure 4(e), the deformation of rectangular design is lower than those of other design. From these results, it can be concluded that the semicircle and multi-stage design can increase the structural deformation. The increment of structural deformation also results in the improvement of stroke efficiency as shown in Figure 4(f). From the results, the design of round shape and multi-stage can enhance the stroke efficiency.

From the above results, it can be seen that each design reveals various strengths and weaknesses of the crashworthiness criteria. To clearly identify the overall performance score and ranking of each design, the technique of order of preference by similarity to ideal solution (TOPSIS) discussed in previous section is performed. Firstly, the decision matrix is constructed from raw data of *EA*, *SEA*, F_{max} , *CFE*, and *SE* as shown in Table 4. Then, the normalized decision matrix is estimated as presented in Table 5. Next step, the weighted normalized decision matrix is established as shown in Table 6. From all five criteria, the weightage is set to be 1/5. *EA*, *SEA*, *CFE*, and *SE* are defined as the advantageous index while F_{max} is the negative effect of impact. Thus, the maximum values of *EA*, *SEA*, *CFE*, and *SE* are defined to be the ideal best and their minimum values are set to be the ideal worst. On the other hand, the lowest value of F_{max} is determined to be the ideal best and its maximum value is defined to be the ideal worst. Then, the Euclidean distance from ideal best and worst is calculated as presented in Table 7. After obtaining the Euclidean distance, the performance score is calculated for each design. The performance score and ranking results are shown in Table 8. The results show that the triple stage UPD guard bar yield the best performance score. The double stage UPD guard bar possesses the second ranking while the semicircle UPD guard bar and rectangular UPD guard bar are the third and fourth ranking, respectively. Based on the overall performance score, the triple stage design can improve the crashworthiness up to 10% while the double stage design can enhance about 5.1% as compared with the rectangular design

of standard UPD guard bar. Besides, the semicircle design shows higher overall performance score than rectangular design but not much significant difference since both designs are single stage impact absorption type. From the section, it can be concluded that the design of multi-stage and round shape outer part can improve the overall crashworthiness score up to 10%.

Table 4: Decision matrix for TOPSIS

Design Number	Decision Criteria				
	<i>EA</i> (J)	<i>SEA</i> (J/kg)	F_{max} (kN)	<i>CFE</i>	<i>SE</i>
1	552.47	547	64.19	0.29	0.52
2	534.02	528.73	42.94	0.13	0.95
3	614.47	379.30	30.99	0.17	0.77
4	676.33	301.93	21.63	0.16	0.94

Table 5: Normalized decision matrix for TOPSIS

Design Number	Normalized Decision Criteria				
	<i>EA</i> (J)	<i>SEA</i> (J/kg)	F_{max} (kN)	<i>CFE</i>	<i>SE</i>
1	0.463	0.606	0.747	0.746	0.321
2	0.447	0.586	0.499	0.332	0.584
3	0.515	0.420	0.360	0.419	0.473
4	0.566	0.335	0.252	0.398	0.577

Table 6: Weighted normalized decision matrix for TOPSIS

Design Number	Weighted Normalized Decision Criteria				
	<i>EA</i> (J)	<i>SEA</i> (J/kg)	F_{max} (kN)	<i>CFE</i>	<i>SE</i>
1	0.093	0.121	0.149	0.149	0.064
2	0.090	0.117	0.010	0.067	0.117
3	0.103	0.084	0.072	0.084	0.095
4	0.113	0.067	0.050	0.080	0.115
Ideal best	0.113	0.121	0.050	0.149	0.117
Ideal worst	0.090	0.067	0.149	0.067	0.064

Table 7: Euclidean distance from the ideal best and worst matrix for TOPSIS

Design Number	Euclidean Distance From	
	Ideal Best	Ideal Worst
1	0.114	0.099
2	0.100	0.088
3	0.082	0.088
4	0.088	0.115

Table 8: The performance score and ranking for TOPSIS

Design Number	Performance Score	Ranking
1	46.5%	4
2	46.9%	3
3	51.6%	2
4	56.5%	1

7 Conclusions

Various designs of UPD guard bar is investigated in this paper, in order to improve the crashworthiness under impact. The dynamic drop impact experiment is performed in explicit finite element code LS-dyna. The obtained results can be concluded that the increment of structural stage can improve the energy absorbing capability. However, as the number of stages increases, the specific energy absorption trends to decrease because of the increment of its mass. Moreover, the design with round shape outer part and the increment of the number of stages can significantly minimize the peak crash force and improve the stroke efficiency.

By using TOPSIS to perform multi-criteria decision analysis method, the results indicate that the triple stage UPD guard bar yields the best performance score. The double stage, semicircle, rectangular design acquires the second, third and fourth order of performance score, respectively. The triple stage design can improve the crashworthiness up to 10% while the double stage design can enhance about 5.1% as compared with the rectangular design of standard UPD guard bar.

Acknowledgments

This research was funded by King Mongkut's University of Technology North Bangkok. Contract no. KMUTNB-62-NEW-08.

References

- [1] World Health Organization, "Global status report on road safety time for action," World Health Organization, Geneva, Switzerland, 2009.
- [2] S. Koetniyom, S. Chanthanumataporn, M. Dangchat, S. Pangkreung, and C. Srisurangkul, "Technical effectiveness of ABS, non-ABS and CBS in step-through motorcycles," *Applied Science and Engineering Progress*, to be published. doi: 10.14416/j.asep.2019.11.002.
- [3] Federal Highway Administration "Highway Statistics 2017 - Policy | Federal Highway Administration," Jul. 18, 2018. [Online]. Available: <https://www.fhwa.dot.gov/policyinformation/statistics/2017/>
- [4] D. Juodvalkis, J. Sapragonas, and P. Griškevičius, "Effects of spot welding on the functionality of thin-wall elements of car's deformation zone," *Mechanika*, vol. 77, no. 3, pp. 34–39, 2009, doi: 10.5755/j01.mech.77.3.15229.
- [5] B. S. Bloch, "Improved crashworthy designs for truck underride guards," presented at the 16th International Technical Conference on the Enhanced Safety of Vehicles in Windsor, Ontario, Canada, Oct. 1998.
- [6] D. Dailionis and P. Griškevičius, "Crashworthiness simulations of side underrun protection devices," in *Proceedings of 15th International Conference. Mechanika*, Jan. 2010, pp. 131–134.
- [7] European Union, "Europa Summaries of EU legislation," European Union, Bruxelles, Belgium, 2019.
- [8] NHTSA, "FMVSS No. 223 Rear impact guards and FMVSS No. 224 Rear impact protection," 2016. [Online]. Available: http://annaleahmary.com/wordpress/wp-content/uploads/2016/06/Preliminary_Regulatory_Evaluation_-_Re_NPRM_published_Dec_16_2015-1.pdf.
- [9] United Nations Economic Commission for Europe, "UNECE No. 58 - Rear underrun protective devices (RUPDs)," United Nations Economic Commission for Europe, Geneva, Switzerland [Online]. Available: <https://www.unece.org/fileadmin/DAM/trans/main/wp29/wp29regs/r058r2e.pdf>
- [10] Z. F. Albahash and M. N. M. Ansari, "A review on rear under-ride protection devices for trucks," *International Journal of Crashworthiness*, vol. 22, no. 1, pp. 95–109, 2017.
- [11] J. Mariolani, A. De Arruda, and L. Schmutzler, "Development of new underride guards for enhancement of compatibility between trucks and cars," presented at the Proceedings of 17th International Technical Conference on the Enhanced Safety of Vehicles, Amsterdam, Netherlands, 2001.

- [12] M. Soltani, T. B. Moghaddam, M. R. Karim, and N. H. Ramli Sulong, “Analysis of developed transition road safety barrier systems,” *Accident Analysis & Prevention*, vol. 59, pp. 240–252, Oct. 2013, doi: 10.1016/j.aap.2013.05.029.
- [13] L. Hong-fei, P. Tao, X. Hong-guo, T. Li-dong, and S. Li-li, “Research on the intelligent rear under-run protection system for trucks,” in *2010 8th World Congress on Intelligent Control and Automation*, Jul. 2010, pp. 5274–5278, doi: 10.1109/WCICA.2010.5554843.
- [14] J. Framby and D. Lantz, “Robustness and Reliability of Front Underrun Protection Systems,” M.S. thesis, Chalmers University of Technology, Göteborg, Sweden, 2010.
- [15] P. Galipeau-Bélair, “Design and development of side underride protection devices (SUPD) for heavy vehicles,” M.S. thesis, University of Ontario Institute of Technology, 2014.
- [16] Z. F. Al-Bahash, M. N. M. Ansari, and Q. H. Shah, “Design and simulation of a rear underride protection device (RUPD) for heavy vehicles,” *International Journal of Crashworthiness*, vol. 23, no. 1, pp. 47–56, Jan. 2018, doi: 10.1080/13588265.2017.1302040.
- [17] L. Xue and J. Yang, “A study on the application of energy-dissipating protection device in car-to-truck rear underride,” in *2013 Fifth International Conference on Measuring Technology and Mechatronics Automation*, Jan. 2013, pp. 130–134, doi: 10.1109/ICMTMA.2013.43.
- [18] G. Rechnitzer, C. T. Powell, and K. A. Seyer, “Development and testing of energy absorbing rear underrun barriers for heavy vehicles,” presented at the National Highway Traffic Safety Administration, Washington, DC, USA 1996.
- [19] B. S. Min and J. U. Cho, “Impact characteristic according to the structure of crash box at the vehicle,” *Archives of Metallurgy and Materials*, vol. 62, no. 2B, 2017, doi: 10.1515/amm-2017-0151.
- [20] D. F. M. Silva, C. M. A. Silva, I. M. F. Bragança, C. V. Nielsen, L. M. Alves, and P. A. F. Martins, “On the performance of thin-walled crash boxes joined by forming,” *Materials (Basel)*, vol. 11, no. 7, Jun. 2018, doi: 10.3390/ma11071118.
- [21] H. R. Zarei and M. Kröger, “Optimization of the foam-filled aluminum tubes for crush box application,” *Thin-Walled Structures*, vol. 46, no. 2, pp. 214–221, Feb. 2008, doi: 10.1016/j.tws.2007.07.016.
- [22] F. Usta and H. S. Türkmen, “Experimental and numerical investigation of impact behavior of nested tubes with and without honeycomb filler,” *Thin-Walled Structures*, vol. 143, p. 106256, Oct. 2019, doi: 10.1016/j.tws.2019.106256.
- [23] C.-L. Hwang, Y.-J. Lai, and T.-Y. Liu, “A new approach for multiple objective decision making,” *Computers and Operations Research*, vol. 20, no. 8, pp. 889–899, Oct. 1993, doi: 10.1016/0305-0548(93)90109-V.
- [24] C.-L. Hwang and K. Yoon, *Multiple Attribute Decision Making: Methods and Applications A State-of-the-Art Survey*. Berlin, Germany: Springer-Verlag, 1981.
- [25] W. Meethom and N. Koohathongsumrit, “An integrated potential assessment criteria and topsis based decision support system for road freight transportation routing,” *Applied Science and Engineering Progress*, to be published, doi: 10.14416/j.ijast.2019.01.002.